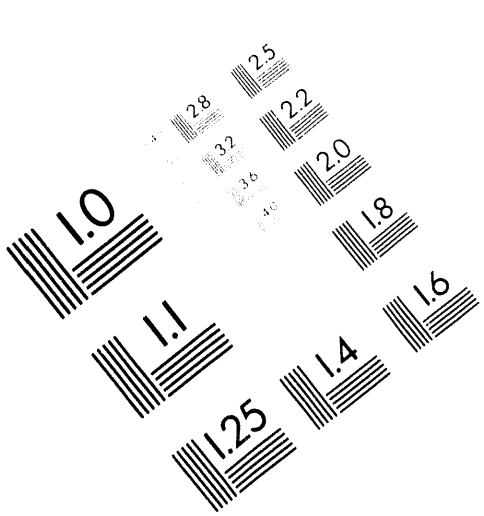

Association for Information and Image Management

1100 Wayne Avenue, Suite 1100
Silver Spring, Maryland 20910

301/587-8202

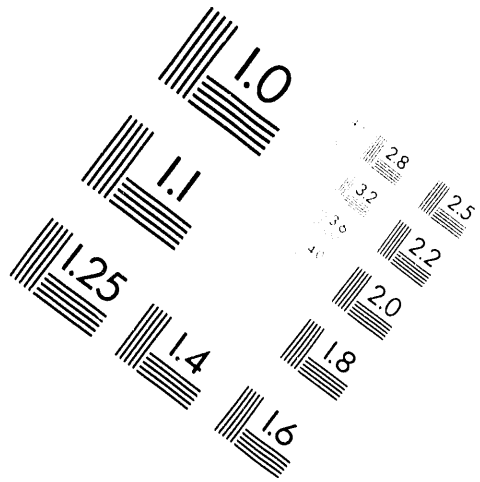

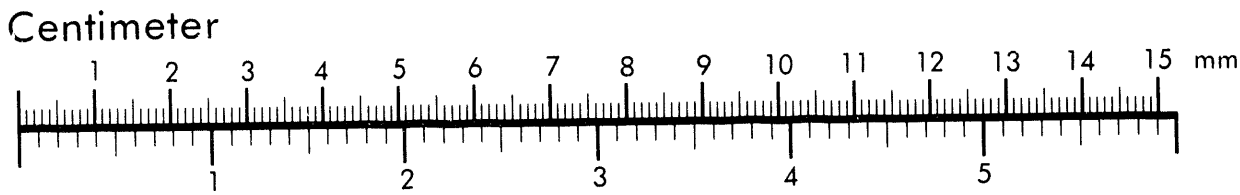

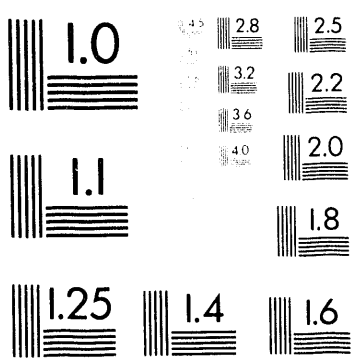

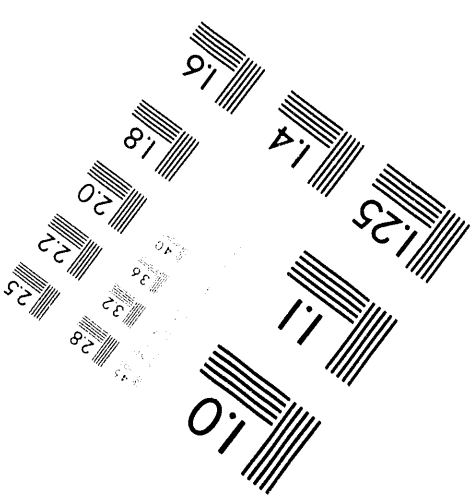

MANUFACTURED TO AIIM STANDARDS
BY APPLIED IMAGE, INC.

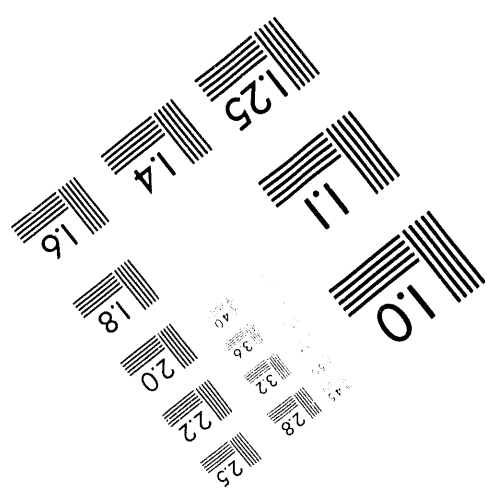

1 of 1

10/6-17-94 SCC

Conf-940233--1

SLAC-PUB-6477
April 1994
T/E

Hard Diffraction and Deep Inelastic Scattering*

J. D. BJORKEN

Stanford Linear Accelerator Center

Stanford University, Stanford, California 94309

ABSTRACT

Talk given at the
International Workshop on Deep Inelastic Scattering and Related Subjects
February 6–11, 1994
Eilat, Israel

* Work supported by the Department of Energy, contract DE–AC03–76SF00515.

1. Introduction: What is Hard Diffraction?

Since the advent of hard-collision physics, the study of diffractive processes—"shadow physics"—has been less prominent than before. However, there is now a renewed interest in the subject, especially in that aspect which synthesizes the short-distance, hard-collision phenomena with the classical physics of large rapidity-gaps. This is especially stimulated by the recent data on deep-inelastic scattering from HERA, as well as the theoretical work which relates to it.

The word "diffraction" is sometimes used by high-energy physicists in a loose way. So I here begin by defining what I mean by the term:

A diffractive process occurs if and only if there is a large rapidity gap in the produced-particle phase space which is not exponentially suppressed.

Here a rapidity gap means essentially *no* hadrons produced into the rapidity gap (which operates in the "lego" phase-space of pseudo-rapidity and azimuthal angle). And non-exponential suppression implies that the cross-section for creating a gap with width $\Delta\eta$ does not have a power-law decrease with increasing subenergy $\hat{s} = e^{\Delta\eta}$, but behaves at most like some power of pseudorapidity $\Delta\eta \sim \log \hat{s}$.

The term "hard diffraction" shall simply refer to those diffractive processes which have jets in the final-state phase-space. We may also distinguish, if desired, two subclasses, as suggested by Ingelman: [1]

i) Diffractive hard processes have jets on only one side of the rapidity gap.

ii) Hard diffractive processes have jets on both sides of the rapidity gap.

2. Reggeons and Pomerons

Rapidity gap processes are conveniently described in the language of complex angular-momentum theory, *i.e.* Regge-pole theory and its generalizations [2]. While this subject is not very much in fashion, there is no reason for this. Its foundations are as solid as QCD itself. The Regge phenomenology for deep-inelastic scattering is in fact not too unfamiliar. The basic results are contained in the properties of the moments of the structure functions

$$M(n,Q^2) = \int_0^1 dx\, x^{n-1} F_2(x,Q^2)\ . \tag{1}$$

For $\mathrm{Re}\, n$ large enough $M(n,Q^2)$ clearly exists. As $\mathrm{Re}\, n$ decreases, eventually M becomes singular. It turns out that this singularity can typically be identified with the analytically continued angular momentum $J(t)$ of the system which is exchanged between the virtual photon and the nucleon. (Recall that F_2 represents the absorptive part of the forward elastic scattering amplitude of the virtual photon from the nucleon.) The relationship is

$$n = J(0) - 1\ . \tag{2}$$

For example, for $I = 1$ exchange (relevant for the nonsinglet structure function $F_{2p} - F_{2n}$), the exchanged object is the ρ and its orbital excitations. The angular momentum versus mass (or t) is exhibited in Fig. 1. From experiment, one knows quite accurately J versus t and

$$J(0) = 0.45\ . \tag{3}$$

For a clean two-body bound state, the singularity in the n-plane of $M(n,Q^2)$ is in

fact a pole, so that as $n \to J(0)$

$$M(n,Q^2) \to \frac{\beta_\gamma(Q^2)\beta_{\mathrm{nucleon}}}{n - J(0)} \tag{4}$$

and

$$F_2 \to x^{1-J(0)}\ . \tag{5}$$

In this case it is essential to realize that the location of the singularity is independent of Q^2; in fact the coefficient must factorize into the product of the coupling of nucleon to Reggeon, and of the Q^2-dependent photon-Reggeon coupling.

The physics of the singularity corresponding to "singlet exchange" is less clear. However Donnachie and Landshoff [3] do quite well in assuming a pole singularity in the n-plane (or better, J-plane) at $n = 0.08$, as well as factorization of the residues. Indeed they argue that this exchanged object, the "soft Pomeron," couples to consistent quarks in a simple way. However the dependence of J upon t (or M^2) is known to be quite different (cf. Fig. 1) than for the ordinary Reggeons, suggesting a distinctly different dynamical origin.

While the "soft-Pomeron" exchange describes photoproduction and hadron-hadron collisions well, it fails to describe the sharp rise of F_2 at small x and large Q^2 seen at HERA. Here the structure anticipated from perturbative QCD [4], the "BFKL Pomeron," is the prime candidate. This singularity is not a pole but a cut in the n plane, starting at

$$n = +\omega_p \tag{6}$$

with

$$\omega_p = \frac{12\alpha_s \ell n\, 2}{\pi} \approx 0.4\ . \tag{7}$$

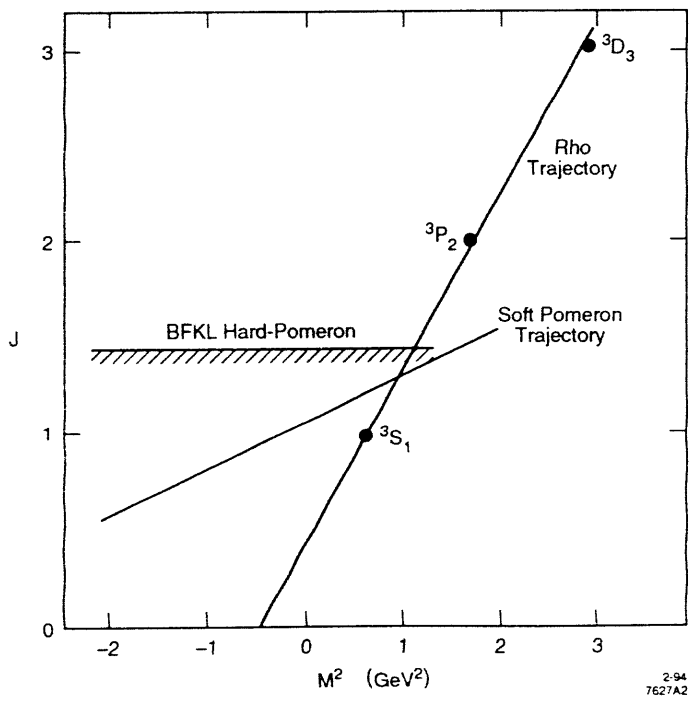

Figure 1. Regge trajectories: J versus M^2 for the ρ, the "soft Pomeron", and the "perturbative Pomeron."

The behavior predicted for $F_2(x)$ is

$$F_2 \sim \frac{x^{-\omega_p}}{\sqrt{\ell n(1/x)}} \tag{8}$$

leading to

$$M(n,Q^2) \sim \frac{M(Q^2)}{\sqrt{(n-\omega_p)}} \,. \tag{9}$$

Note that ω_p may depend upon Q^2; there is no contradiction with general Regge theory because the singularity is a cut, not a pole.

The physics of the BFKL Pomeron is glorified 2-gluon exchange: roughly speaking (and *only* roughly) it is exchange of a gluon ladder. The physics of the ordinary Reggeon (such as the ρ) is exchange of a ladder, for which the sides are generally regarded to be constituent quarks. The rungs of the ladder represent the binding potential between quarks (non-perturbative gluons?).

The physics of the "soft-Pomeron" is much less clear. Most theorists nowadays also consider it as derived from two-gluon exchange [5]; indeed in principle it need not be a singularity distinct from the BFKL singularity. But if soft and BFKL Pomerons have a common origin, the discontinuity across the cut in the n-plane must have a quite strong Q^2 dependence (cf. Fig. 2); it will be a challenge to theory to exhibit how this comes about.

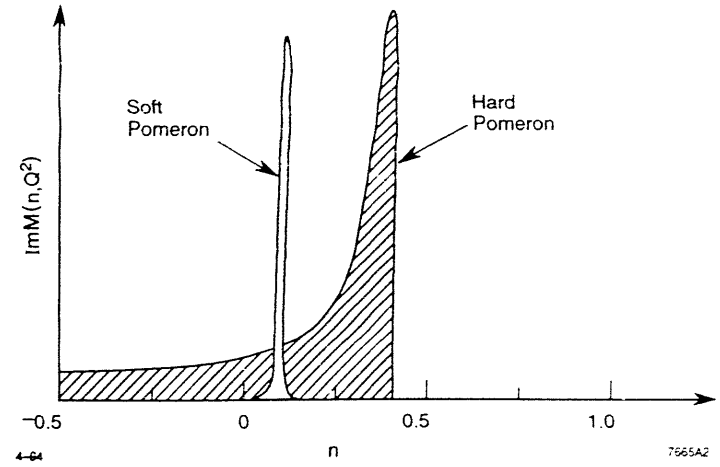

Figure 2. Schematic of the discontinuity across the n-plane (or J-plane) singularities for soft and hard Pomerons.

An alternative view which in my opinion is also worth consideration [6] is

that the soft Pomeron has little to do with gluons but much to do with constituent quarks and the spontaneously broken chiral phase of QCD. Manohar and Georgi [7] have argued that at energy scales below 1 GeV (distance scales greater than 0.2f), the appropriate description of the strong interaction is an effective action built of constituent quarks, Goldstone pions, and a small amount of gluons. Such a picture is motivated by the success of the additive quark model for spectroscopy and soft-collision dynamics, as well as by the small size of the constituent quarks (as measured by $\sigma_{qq} \sim 4\ mb$). It is certainly not obvious that the Manohar-Georgi effective action is capable of producing the needed soft-Pomeron s-dependence. If so, I would suspect that the (quite old-fashioned) ladders with pions (and σ?) as elements (cf. Fig. 3) have to be main ingredients in building up such a Pomeron. A fresh look at this very old question may be of use.

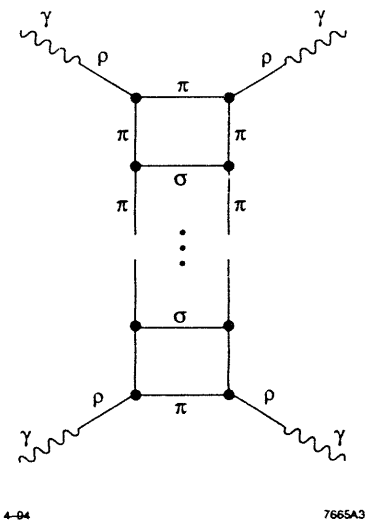

Figure 3. Soft-Pomeron forward scattering amplitude for scattering of real photons.

3. The S-Channel View of Hard Diffraction

Traditionally ladder-exchanges are best described in t-channel Regge terms. But it seems to be the case that most—but not all—of the physics of the perturbative BFKL Pomeron is more transparent in s-channel language. This is especially evident of the work of Nikolaev and Zakharov [8], and of Mueller [9]. The reason for this can be traced back to the basics of light-cone quantization [10]. For diffractive processes there always exists a reference frame such that zero pseudorapidity occurs in the center of the rapidity gap. Consequently in such a frame all final-state particles have small production angles; they are unambiguously either left-movers or right-movers. This will be true at the parton level as well: wee partons play a relatively inconsequential role.

In perturbative QCD, as in QED, the essential interaction between the left-movers and right-movers will be *instantaneous* Coulomb gluon-exchange. The dynamics is the Coulomb interaction. During this interaction the number and impact parameters of the incident partons do *not* change. Most complications are associated with the formation of the parton configurations. With the exception of effects related to ultraviolet-divergence renormalizations, these occur on a long (time-dilated) time scale.

Because impact-parameter is conserved during the collision (impact-parameter is the high energy limit of orbital angular momentum), it is advantageous to Fourier-transform out of transverse-momentum space and into impact-space as much as possible. It is also convenient to use color singlet projectiles as well, so that the basic interaction is between color-dipoles. We shall hereafter consider scattering of a virtual, highly spacelike photon on another less virtual, but spacelike photon. The process is double pair production of quarks $Q\overline{Q}$ and $q\bar{q}$ via single

gluon exchange. The amplitude in impact space is easily written down (cf. Fig. 4 for some notation)

$$T(Q,\overline{Q}|q,\overline{q}) = \Psi(Q,\overline{Q},z_\ell)V(Q,\overline{Q}|q,\overline{q})\psi(q,\overline{q},z_r)\ . \tag{10}$$

Here, in an obvious notation, $\boldsymbol{Q},\overline{\boldsymbol{Q}},\boldsymbol{q},\overline{\boldsymbol{q}}$ represent impact parameters, not momenta, and z_ℓ, z_r are longitudinal fractions of the quarks. The potential V is a dipole-dipole potential. Recalling that a Coulomb potential in momentum space is

$$V(t) = \frac{4\pi\,\alpha_s}{t} \tag{11}$$

and that the Fourier transform of such a V is a logarithm

$$V(b) = \int \frac{d^2k}{(2\pi)^2}\, e^{i\boldsymbol{k}\cdot\boldsymbol{b}} \cdot \frac{4\pi\alpha_s}{k^2} = -\alpha_s \ell n\, b^2 \tag{12}$$

we get for the dipole-dipole force

$$\begin{aligned} V(Q,\overline{Q}|p,\overline{p}) &= \alpha_s[\ell n(Q-q)^2 + \ell n(\overline{Q}-\overline{q})^2 - \ell n(Q-\overline{q})^2 - \ell n(\overline{Q}-q)^2] \\ &\Rightarrow 2\alpha_s(\boldsymbol{Q}-\overline{\boldsymbol{Q}})\cdot\left[\frac{(\overline{\boldsymbol{q}}-\boldsymbol{Q})}{(\overline{\boldsymbol{q}}-\boldsymbol{Q})^2} - \frac{(\overline{\boldsymbol{q}}-\boldsymbol{Q})}{(\overline{\boldsymbol{q}}-\boldsymbol{Q})^2}\right] \end{aligned} \tag{13}$$

where the last step is appropriate if $(\boldsymbol{Q}-\overline{\boldsymbol{Q}})^2 \ll (\boldsymbol{q}-\overline{\boldsymbol{q}})^2$.

For the latter case we can expect a pair of left-moving, nearly balanced high-p_T dijets with $p_t^2 \sim (Q-\overline{Q})^{-2}$. On the other hand, if there is a close collision, say, between Q and q, because

$$(Q-q)^2 \ll (\overline{Q}-\overline{q})^2 \sim (\overline{Q}-q)^2 \sim (Q-\overline{q})^2 \sim R. \tag{14}$$

then

$$V(Q,\overline{Q}) \simeq \alpha_s \ell n\, \frac{(Q-q)^2}{R^2} \tag{15}$$

and the process is just quark-quark "Coulomb"-scattering from the contents of

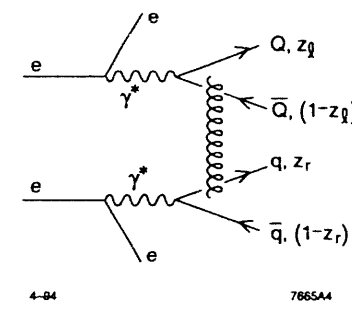

Figure 4. Double pair production via gluon exchange in the collision of two spacelike virtual photons.

somewhat "resolved" virtual photons (cf. Fig. 5), leading to nearly coplanar dijets with a large rapidity interval between them.

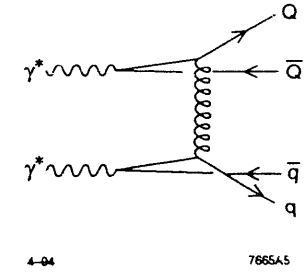

Figure 5. "Coulomb" interaction of two quarks via single gluon exchange.

We do not detail the nature of the wave functions (basically Fourier transforms of old-fashioned-perturbation-theory energy denominators); this can be found elsewhere [8,11]. We do however make mention of color-factors. In what follows, it will be useful *not* to sum colors early. A good rule is to specify the color of each outgoing quark (as opposed to antiquark) and the color of the quark-index of each

outgoing gluon. Once the color-flow diagram for the amplitude is drawn, the colors of outgoing "antiquark" lines are fixed. When we deal with multigluon final states these details will be very important.

So far, constructing the impact-space amplitude does not look too vital. However when one considers multigluon production the benefits multiply. In any case, to go back to a momentum-space amplitude one writes

$$\tilde{T}(P,\overline{P},p,\overline{p}) = \int \frac{d^2\overline{Q}\,d^2q\,d^2\overline{q}}{(2\pi)^6}\, e^{i(\overline{P}\cdot\overline{Q}+p\cdot q+\overline{p}\cdot\overline{q})} T(0,\overline{Q},q,\overline{q}) \ . \tag{16}$$

Setting $Q = 0$ and not integrating over P avoids extraneous δ-functions and/or areas of the universe. Evidently momentum conservation is implied, so

$$P + \overline{P} + p + \overline{p} = 0 \ . \tag{17}$$

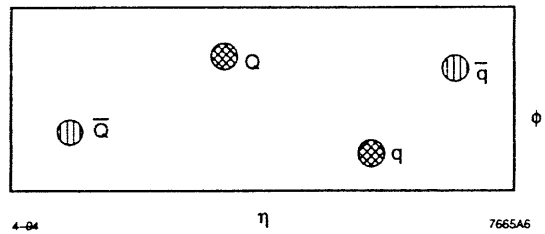

Figure 6. Final-state configuration corresponding to the process in Fig. 5.

We now consider a simple hard-diffraction process, corresponding to the final state shown in Fig. 6. A simpler electroweak prototype is obtained by replacing each photon by a W^+ and considering the Coulomb contribution shown in Fig. 7.

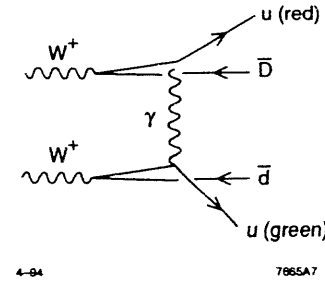

Figure 7. Modification of the process in Fig. 5 by replacement of virtual photons with virtual W's, and the exchanged gluon with an exchanged photon.

The final state morphology is clearly what is shown in Fig. 8 and the amplitude in impact space is just

$$T = \frac{4}{9}\alpha \cdot \psi(Q,\overline{Q})\ell n\left[\frac{(Q-\overline{Q})^2}{R^2}\right]\psi(p,\overline{p}) \ . \tag{18}$$

Hadronization, according to the "antenna rules," is localized to the regions allowed by the radiation from the color dipoles. This is to be contrasted with the hadronization from single gluon exchange, most conveniently described in terms of a "double-sided lego plot" (Figs. 9 and 10) [12].

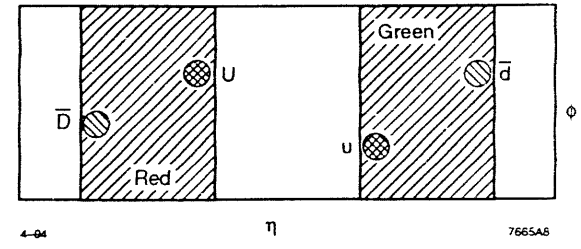

Figure 8. Final state hadronization appropriate to the process in Fig. 7. The red color dipole radiates gluons (and hadrons) only into the phase-space labeled "Red."

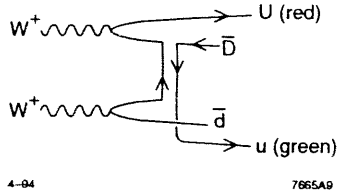

Figure 9. Color-flow diagram corresponding to the strong process in Fig 5.

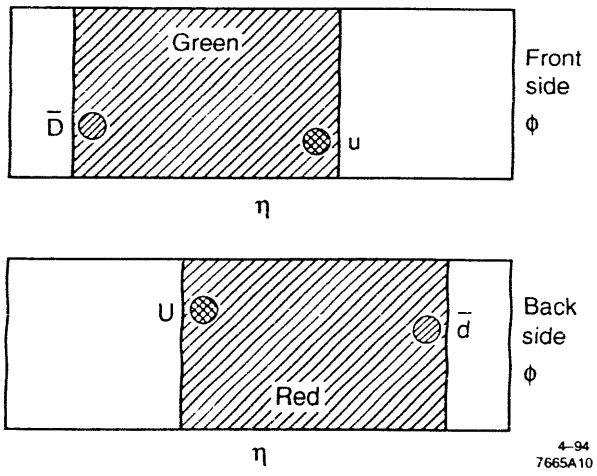

Figure 10. "Double-sided" lego plot describing the hadronization from the strong Coulomb-gluon exchange process down in Fig. 9. In the large N_c limit the contributions from front and back sides are incoherently added.

In order to obtain a QCD diffractive amplitude, two Coulomb gluons must be exchanged. In impact-space, this is immediate. In order to restore the color singlet structure, both gluons must be exchanged between the quarks; thus the replacement is simply (cf. Fig. 11)

$$V = \alpha_s \ell n \, \frac{(Q-q)^2}{R^2} \Rightarrow \left[\alpha_s \ell n \, \frac{(Q-q)^2}{R^2} \right]^2 . \qquad (19)$$

The final-state morphology of this two-gluon exchange process should be essentially the same as that for the photon exchange process illustrated in Fig. 7 and 8. The nonlocality of the two-gluon system is limited to a small space-time region; there is no large "antenna" available to produce leading-log soft radiation. This assertion has been in fact checked by Zeppenfeld [13].

In any case, to logarithmic accuracy, $\alpha_s \sim \log^{-1}$ so that Eq. (19) implies that the single-gluon exchange amplitude is modified by a *constant* factor [α_s log]. Thus the *ratio* of the cross-section with gap to the cross-section without gap should not depend on the external details of positions and transverse momenta of tagging-jets unless there is a gross change in the external parameters relative to what we specified [14]. The result is roughly, when the color factors, etc., are more carefully considered

$$\frac{\sigma_{\text{gap}}}{\sigma_{\text{no gap}}} \approx 0.1 \ \langle |S|^2 \rangle \qquad (20)$$

with $\langle |S|^2 \rangle$ an absorption correction arguably not too important for this case [15].

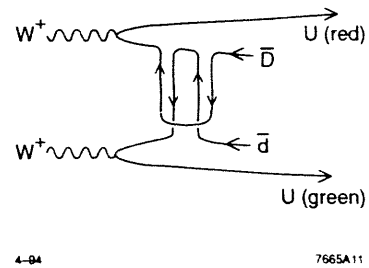

Figure 11. Color-flow structure of the two-gluon-exchange amplitude.

Gross changes in the external parameters, however, can be of interest. If we change the kinematics to what was discussed at Eq. (13), where $(Q-\overline{Q})^2 \ll (q-\overline{q})^2$,

then the exchanged gluon sees a small $Q\overline{Q}$ color dipole, and the modification is

$$V = \alpha_s(\boldsymbol{Q} - \overline{\boldsymbol{Q}}) \cdot \boldsymbol{d} \quad \Rightarrow \quad V^2 = \left[\alpha_s(\boldsymbol{Q} - \overline{\boldsymbol{Q}}) \cdot \boldsymbol{d}\right]^2 . \tag{21}$$

where d is the (large) dipole-moment provided by q and $\overline{q}$. The ratio of second-order to first-order amplitudes is *suppressed* by a factor

$$\alpha_s(\boldsymbol{Q} - \overline{\boldsymbol{Q}}) \cdot \boldsymbol{d} \approx \alpha_s \left|\frac{p_t}{P_t}\right| \tag{22}$$

where $P_t^2 \sim (Q - \overline{Q})^{-2} \gg p_t^2 \sim (q - \bar{q})^{-2}$. Consequently

$$\frac{\sigma_{\text{gap}}}{\sigma_{\text{no gap}}} \approx \alpha_s^2 \, \frac{p_t^2}{P_t^2} \tag{23}$$

is power-law suppressed. This is actually very relevant to the HERA processes. The above argument is due to Collins, Frankfurt, and Strikman [16], and detailed calculations are provided by Donnachie and Landshoff [17].

But within these caveats, the proportionality of two-gluon and one-gluon exchanges argues that (to logarithmic accuracy) the two-gluon-exchange "Pomeron" in general acts the same way as a single gluon. If this is interpreted, as first suggested by Ingelman and Schlein [18], in terms of a "parton-distribution of the Pomeron," it implies [19] there will be a super-hard component $\sim \delta(1 - x)$ or $(1 - x)^{-1}$ corresponding to this notion of "Pomeron = gluon."

4. Multijet Final States

We now generalize these ideas to multigluon final states. Our formalism rests heavily on recent work by Nikolaev, Zakharov, and Zoller [20], Mueller and Patel [21], Del Duca [22], and of course Lipatov [23].

Our goal is to deconstruct the BFKL Pomeron as much as possible. That is, we would like to understand as explicitly as possible the structure in impact-parameter space of the multijet production amplitudes and multijet final states which build the BFKL cross-section. As will become quite obvious, the arguments are still sketchy and far from rigorous. In what follows, we simplify to the large N_c limit of QCD.

We again consider the collision of virtual γ's with production of two pairs of quark-antiquark jets. Now consider the modification of the original amplitude

$$T_0 = \psi(Q, \overline{Q})\, V(Q\overline{Q}|q\overline{q})\, \psi(q, \bar{q}) \tag{24}$$

due to the emission of an extra soft gluon into the middle of the lego plot. We assume "multi-Regge kinematics," *i.e.* that all extra gluons are well-separated from each other in the lego plot, as well as from the leading tagging-jets. They therefore will not influence the conservation of energy and longitudinal momentum. Only transverse momentum balance will matter: we will usually assume all emitted gluons have transverse momenta (and/or impact parameters) comparable in magnitude.

Just as in Weiszacker-Williams QED, the momentum-space amplitude for emission of a soft (left-moving) gluon from a (left-moving) quark is just $\boldsymbol{\epsilon} \cdot \boldsymbol{k}_\perp / k_\perp^2$.

Fourier transformation to impact space leaves this structure the same

$$\int \frac{d^2k}{(2\pi)^2}\,\frac{\epsilon\cdot k}{k^2}\,e^{ik\cdot b} = \frac{-i}{(2\pi)^2}\,\epsilon\cdot\nabla_b \int \frac{d^2k}{k^2}\,e^{ik\cdot b} = \frac{-i}{4\pi}\,\epsilon\cdot\nabla_b \ell n\, b^2 = \frac{-i}{2\pi}\,\frac{\epsilon\cdot b}{b^2}\ . \quad (25)$$

It is therefore clear that the appropriate modification to the impact-space left-moving amplitude is

$$\begin{aligned}\Psi(Q,\overline{Q}) &\Rightarrow \Psi(Q,\overline{Q},g)\,\left[\frac{\epsilon\cdot(g-Q)}{(g-Q)^2} - \frac{\epsilon\cdot(g-\overline{Q})}{(g-\overline{Q})^2}\right] \\ &= \Psi(Q,\overline{Q},g)\,\epsilon\cdot\nabla_g V(Q,\overline{g}|g\overline{Q})\end{aligned} \quad (26)$$

where $g = \overline{g}$ is the transverse coordinate of the gluon. We now scatter this left-moving system with the right-moving system by Coulomb-gluon exchange. There are two ways of doing this corresponding to the gluon jet being either on the front side or the back side of the lego plot. In accordance with Figs. 12 and 13 we obtain two terms. T_{01} has the gluon emitted onto the front side of the lego plot:

$$\begin{aligned}T_{01} &= \Psi(Q,\overline{Q},g)\,V(Q\overline{g}|q\overline{q})\psi(q\overline{q}) \\ &= \Psi(Q\overline{Q})\,\left[\epsilon\cdot\nabla_g V(Q\overline{Q}|g\overline{q})\right]\ V(Q\overline{q}|q\overline{q})\psi(q\overline{q})\ .\end{aligned} \quad (27)$$

The rear-side amplitude T_{10} is (cf. Fig. 13):

$$T_{10} = \Psi(Q,\overline{Q},g)V(g\overline{Q}|q\overline{q})\psi(q\overline{q}) = \Psi(Q\overline{Q})\,\left[\epsilon\cdot\nabla_g V(Q\overline{Q}|q\overline{g})\right]\ V(g\overline{Q}|q\overline{q})\psi(q\overline{q})\ . \quad (28)$$

Notice these two amplitudes will *not* interfere; the color structure of the final states is totally different. This will be true in general and leads to important differences from the structure of QED intermediate states.

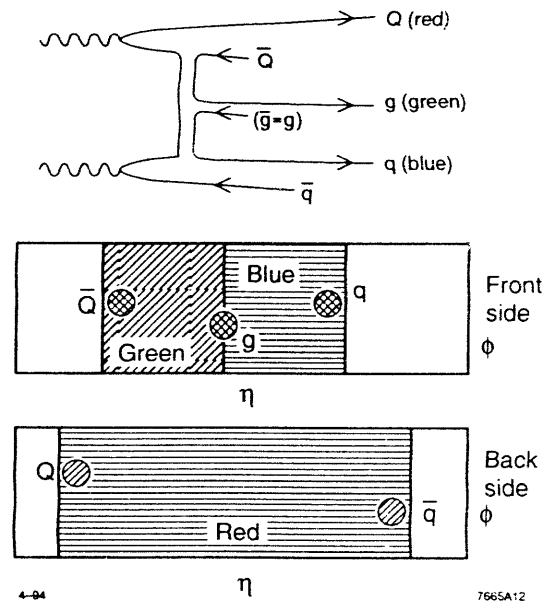

Figure 12. Color-flow diagram for single-gluon production: structure of the lego plot.

Note also that in the above expressions for T_{10} and T_{01} we have considerable symmetry. It should be the case that we get the same answer no matter whether g is associated with the wave function of the right-moving system or the left-moving system. While it is tempting to assume that a parts-integration allows the gradient operation $\epsilon\cdot\nabla_g$ to be performed either to the right or to the left, this is not quite the case.

The residual dependence is probably compensated by similar dependencies of virtual corrections. We set this problem aside; regrettably the virtual-correction issue is beyond the scope of this talk.

In any case, when we generalize to production of n gluons a different formal

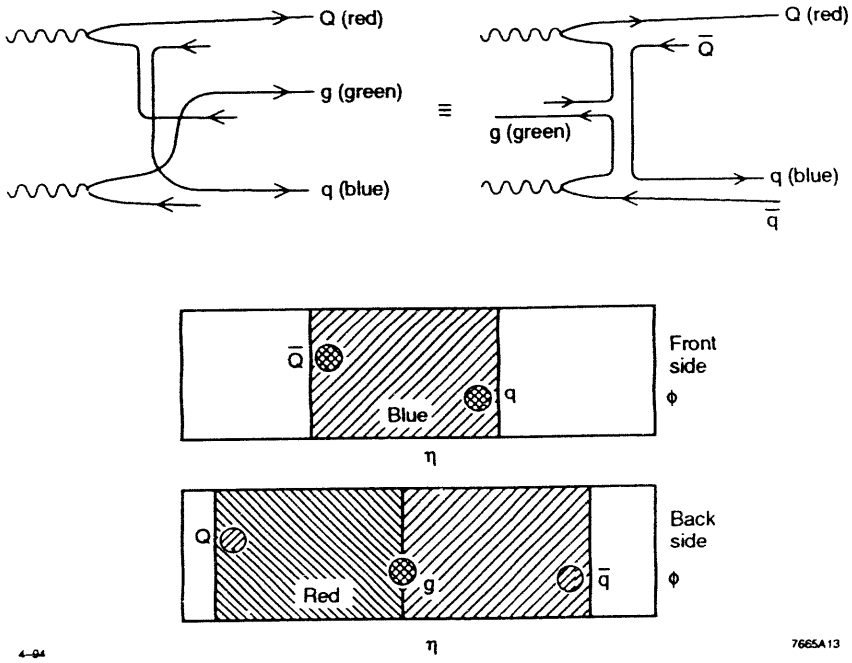

Figure 13. The amplitude for gluon g emitted onto the rear of the lego plot.

structure is convenient. We consider the transverse x, y plane to be the complex plane, and replace the impact parameter $\boldsymbol{b}$ by its complex representation

$$\boldsymbol{b}(x,y) \Rightarrow (x+iy) \equiv b \tag{29}$$

with

$$b^* = (x-iy)\,. \tag{30}$$

Then for a circularly polarized gluon our generic "antenna amplitude" is simply

$$\boldsymbol{\epsilon}\cdot\boldsymbol{\nabla}V = \frac{\boldsymbol{\epsilon}\cdot\boldsymbol{b}}{|\boldsymbol{b}|^2} - \frac{\boldsymbol{\epsilon}\cdot\boldsymbol{b}'}{|\boldsymbol{b}'|^2} = \frac{1}{b} - \frac{1}{b'} = \frac{(b-b')}{bb'}\,. \tag{31}$$

If the other circular polarization is chosen, then one simply complex-conjugates the expression. But in general none of the multigluon amplitudes we consider will interfere with any other multigluon amplitude. So only one convenient polarization need be chosen, as long as one remembers at the appropriate times a factor 2 for sum over polarizations as well as the factor 3 for the sum over colors.

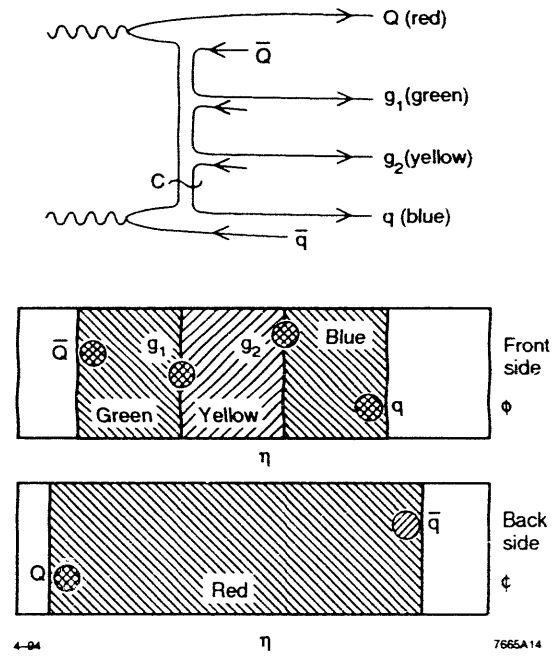

Figure 14. Two-gluon emission amplitude.

Upon writing down T_{02} (cf. Fig. 14, and recognize that $g = \bar{g}$) we see a pattern

of cancellation emerge:

$$
\begin{aligned}
T_{02} &= \Psi(Q\overline{Q})\left[\epsilon\cdot\nabla_1 V(Q\overline{Q}|g_1,\overline{q})\right]\left[\epsilon\cdot\nabla_2 V(Q\overline{g}_1|g_2\overline{q})\right] V(Q\overline{g}_2|q\overline{q})\psi(q\overline{q}) \\
&= \Psi(Q\overline{Q})\left(\frac{1}{Q-g_1}-\frac{1}{\overline{Q}-g_1}\right)\left(\frac{1}{(Q-g_2)}-\frac{1}{(g_1-g_2)}\right) V(Q\overline{g}_2|q\overline{q})\psi(q\overline{q}) \\
&= \Psi(Q\overline{Q})\,\frac{(Q-\overline{Q})}{(Q-g_1)(g_1-g_2)}\,V(Q\overline{g}_2|q\overline{q})\psi(q\overline{q})
\end{aligned}
\tag{32}
$$

and evidently

$$
T_{0n} = \Psi(Q\overline{Q})\,\frac{(Q-\overline{Q})V(Q\overline{g}_n|q\overline{q})}{(\overline{Q}-g_1)(g_1-g_2)\ldots(g_{n-1}-g_n)}\,\psi(q\overline{q})\ . \tag{33}
$$

There is only one simple denominator-factor for each color-dipole associated with the front side of the lego plot [24]. This simplification allows an easy generalization for inclusion of gluons emitted onto the back of the lego plot as well. For example for emission of one gluon on the backside, with rapidity between the first and second of two front-side gluons, we get

$$
\begin{aligned}
T_{12} &= \Psi(Q\overline{Q})\left[\frac{\partial}{\partial f_1}V(Q\overline{Q}|f_1\overline{b})\right]\left[\frac{\partial}{\partial\overline{b}}V(Q\overline{f}_1|f_2\overline{b})\right]\left[\frac{\partial}{\partial f_2}V(b\overline{f}_1|f_2\overline{q})\right] V(b\overline{f}_2|q\overline{q})\psi(q\overline{q}) \\
&= \Psi(Q\overline{Q})\,\frac{(Q-\overline{Q})}{(f_1-Q)(f_1-\overline{Q})}\cdot\frac{(Q-f_1)}{(b-Q)(b-f_1)}\cdot\frac{(b-f_1)}{(b-f_2)(f_1-f_2)} \\
&\quad\times V(b\overline{f}_2|q\overline{q})\psi(q\overline{q}) \\
&= \frac{\Psi(Q\overline{Q})(Q-\overline{Q})V(b\overline{f}_2|q\overline{q})\psi(q,\overline{q})}{[(b-Q)(b-f_2)]\,[(\overline{Q}-f_1)(f_1-f_2)]}\ .
\end{aligned}
\tag{34}
$$

The important feature of this structure is that the answer does not depend upon whether the rapidity of gluon b is large or small compared to f_1—or for that matter f_2. The transverse dynamics on the front of the lego plot is decoupled from the

transverse dynamics on the rear. With this example it should be clear what the general amplitude with m gluons $b_1\ldots b_m$ on the back of the lego plot and n gluons $f_1\ldots f_n$ on the front:

$$
T_{mn} = \frac{\Psi(Q\overline{Q})(Q-\overline{Q})^2 V(b_m\overline{f}_n|q\overline{q})\psi(q\overline{q})}{(Q-\overline{Q})(\overline{Q}-f_1)\ldots(f_{n-1}-f_n)(f_n-b_m)(b_m-b_{m-1})\ldots(b_1-Q)}\ . \tag{35}
$$

This expression is constructed for the case in which all partons except q and $\overline{q}$ are left-movers. We are motivated to describe the more general case, since it would clearly allow generalization of the rapidity gap theorem described in the previous section. This invites the following restructuring

$$
T_{mn} = \frac{\Psi(Q\overline{Q})(\overline{Q}-Q)^2 C(b_m\overline{f}_n|q\overline{q})(q-\overline{q})^2\psi(q\overline{q})}{(Q-\overline{Q})(\overline{Q}-f_1)\ldots(f_n-q)(q-\overline{q})(\overline{q}-b_m)\ldots(b_1-Q)}\ . \tag{36}
$$

The "Coulomb kernel" C which must be inserted, in a reference frame in which $\eta = 0$ lies between gluons $b = b_k, b' = b_{k+1}$ and $f = f_\ell, f' = f_{\ell+1}$ is defined as

$$
C(b,\overline{f}|f',\overline{b}') = \frac{(f'-f)(b'-b)}{(f-b)(f'-b')}\,\log\frac{(b-f')(f-b')}{(f-f')(b-b')} \tag{37}
$$

The final form of the amplitude is thus

$$
T = \Psi(Q,\overline{Q})(Q-\overline{Q})^2 C(b\overline{f}|f'\overline{b}')(q-\overline{q})^2\psi(q,\overline{q})S \tag{38}
$$

where the string function S is just the product of denominator factors around the entire color loop. It is perhaps more suggestive to write

$$
S = \epsilon^{-F} \qquad F = \sum_{i\in\text{ loop}} \ell n(g_i - g_{i+1}) \tag{39}
$$

exhibiting a string-like, nearest-neighbor Coulomb interaction between neighboring gluons in impact space. The "Coulomb operator" C acting on S cuts the single

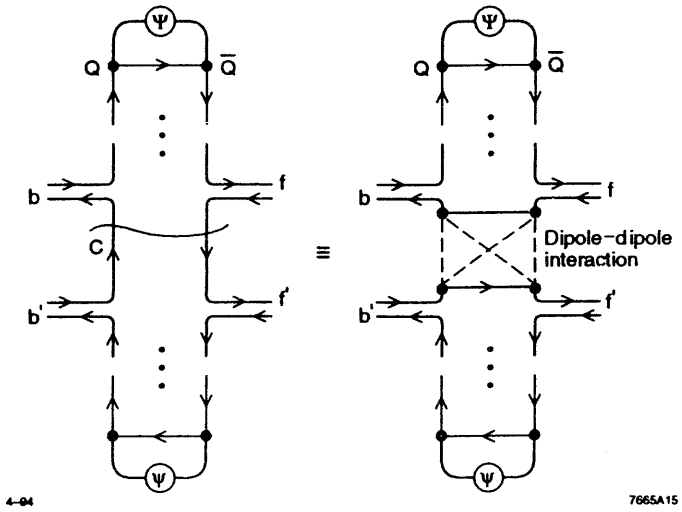

Figure 15. Effect of the Coulomb operator on the "string function."

closed loop into two loops, one left-moving and one right-moving, which locally interact with each other via the dipole-dipole potential (cf. Fig. 15).

Again the structure of Eq. (38) invites the supposition that the amplitude as written does not depend upon which choice of reference frame one makes, *i.e.* which of the gluons are right movers. It is not hard to show that if one changes frames so that one of the gluons, say f, is turned from left-mover into right-mover, then the difference of amplitudes is a total derivative with respect to f. However we have not succeeded in arguing away the surface-term. The omission of virtual corrections is, at the least, one possible reason for the failure.

With all these preliminaries and caveats it is now immediate to generalize the rapidity gap theorem stated in the previous section. The amplitude with one-gluon exchange is of the form

$$T_{mn} = \frac{\Psi(Q\overline{Q})(Q-\overline{Q})^2}{(Q-\overline{Q})(\overline{Q}-f_1)\cdots(f-b)\cdots(b_1-Q)}\left[\alpha_s \log\frac{(b-f')(f-b')}{(f-f')(b-b')}\right] \times\left[\frac{(q-\overline{q})^2\psi(q\overline{q})}{(q-\overline{q})(\overline{q}-b)\cdots(b'-f')\cdots(f_1-q)}\right]. \tag{40}$$

The color structure is totally explicit here, so that it is now trivial to see that just as before, the second gluon is inserted between the interacting left-moving and right-moving dipoles in order to create the gap. Again the result is

$$T_{mn}^{\text{gap}} = T_{mn}^{\text{no gap}} \cdot \left[\alpha_s \ell n\,\frac{(b-f')(f-b')}{(f-f')(b-b')}\right]. \tag{41}$$

Is the argument of the logarithm large or small? For it to be large one pair of partons must have a close encounter while the others do not. From the structure of the amplitude T_{mn}, Eq. (40), it would appear that if Q and $\overline{q}$ are close together while $\overline{Q}$ and q are much further apart then the ratio of the p_t scale on the back side of the lego plot to that on the front will go as the ratio of $|\overline{Q}-q|$ to $|Q-\overline{q}|$. This follows from the scale-invariance of the underlying dynamics. It seems in fact reasonable that most of the time this will be the case and that *on average, it is unlikely that both sides of the lego plot get populated with BFKL jets of comparable* p_t. It will be interesting to examine this assertion in a more quantitative and systematic manner.

In any case, the estimate of rapidity gap fraction made in the previous section can be applied directly here. The ratio of gap-cross-section to that without a gap (for a given *choice* of gap) is

$$\frac{d\sigma_{\text{gap}}(\eta_1\cdots\eta_n, p_{t_1}\cdots p_{t_N})}{d\sigma_{\text{no gap}}(\eta_1\cdots\eta_n, p_{t_1}\cdots p_{t_N})} \sim \alpha_s^2\left\langle \log\frac{p_{\text{t front}}^2}{p_{\text{t rear}}^2}\right\rangle^2. \tag{42}$$

This estimate must still be scrutinized with respect to additional non-perturbative (or higher-order) corrections. We will return to this question later.

We have in this section claimed that these tree-approximation amplitudes build the BFKL cross section. This is an oversimplification, because virtual corrections (in particular ultraviolet renormalizations) have been ignored. We believe these corrections do not greatly modify the conclusions drawn here, because we take ratios of amplitudes to make the argument, and the renormalizations can be expected, to good approximation, to drop out. It is actually very interesting to take the amplitudes as constructed, square them, integrate over gluon phase space and sum over m and n. As is clear from Eq. (35) infinities will occur when impact-parameters of neighboring gluons (on the same side of the lego plot) coincide. A regularization procedure is needed. Nikolaev, Zakharov, and Zoller [20] have introduced a regularization prescription which suffices to produce the energy-dependence of the BFKL cross section. Their regularization is very close to the $(\ )_+$ recipe often used to regularize collinear divergences in the more conventional DGLAP evolution equation [25]. However the corresponding $(\ )_+$ operation is here carried out not in momentum space, but in impact space, and regularizes (box-diagram) ultraviolet divergences.

5. The Nature of the Virtual Photon

In most of the previous discussion we have assumed the applicability of perturbative QCD. This, even for the scattering of spacelike virtual photons from each other, is inadequate. There are good reasons, both experimental and theoretical, for expecting the virtual photon at very small x to have nonperturbative structure. From the experimental side, one sees an A-dependence of deep-inelastic scattering at very small x which goes as $A^{2/3}$, indicative of a nontrivial photon substructure which can be geometrically absorbed on a large nucleus [26]. This is

also a reasonable expectation from the theoretical side [27]. We now review these arguments.

At very small x, generalized vector-dominance arguments, as we used in the previous sections, are correct as a matter of kinematics, not dynamics. The basic issue, as addressed at length in the previous subsection within the context of perturbative QCD, is what constitutes the substructure of the components of the photon wave function on arrival at the target (which here we take as a nucleus, in the fixed-target reference frame). There are two important cases, as we might already anticipate from the discussion in Section 4.

1. *The simpler case:* The photon converts virtually to a symmetric high-p_t $Q\overline{Q}$ pair (plus BFKL extras), which on arrival at the nucleus is a small penetrating color-dipole, and which leaves leading dijets in the lego plot. Such a mechanism leads to a virtual photon cross-section σ_T which scales and is proportional to A:

$$\sigma \sim \alpha_s^2 \cdot \frac{1}{Q^2} \cdot A \ . \tag{43}$$

2. *The less-simple case:* In this case the photon converts virtually to an asymmetric $Q\overline{Q}$ pair; so asymmetric (in z and $(1-z)$) that the Q and $\overline{Q}$ "jets" have $p_T < 1\ GeV$. This configuration is unlikely (the probability is roughly $1\ GeV/Q^2$), but when it does happen there is so much color separation that *non-perturbative* parton evolution occurs between the Q and $\overline{Q}$. On arrival the distribution of partons in the virtual photon, up to a parton energy $\sim (1\ GeV/x)$, is arguably as nonperturbative as those in an ordinary hadron [28]. This is quite sufficient to allow such a virtual photon to be absorbed in nuclear matter in a way not dissimilar to how a ρ or other ordi-

nary hadron is absorbed. The cross-section σ_T in this case is $\pi R^2 \cdot A^{2/3}$, the geometrical cross section, multiplied by $(1\ GeV^2/Q^2)$, the probability of the aligned configuration

$$\sigma_T \sim \left(\frac{M_p^2}{Q^2}\right) \cdot \pi R^2 \cdot A^{2/3} \ . \tag{44}$$

In the generic case, no jets will be seen in the lego plot.

This less-simple case is in fact the vector-dominant description of the final state to be expected in the old-fashioned, pre-QCD parton model. It is still the most reasonable description outside the kinematic region of BFKL enhancement. And even within the BFKL framework discussed in Section 4, the "back side of the lego plot" could still be at—or beyond—the edge of applicability of perturbative QCD when, for example, the p_T of the tagging jets Q and $\overline{q}$ becomes small, but when the p_T of jets $\overline{Q}$ and q remain large.

The best test for distinguishing the two cases is clearly to look for the leading $Q - \overline{Q}$ dijets as tags.

6. Hard Diffraction at HERA

Finally we reach the territory of greatest contemporary experimental interest. There are several mechanisms for diffractive final states in deep-inelastic processes. For the "simple" photon configuration we may entertain the diffractive final states shown in Fig. 16. Cases (a) and (b) are diffractive hard processes; it is reasonable to use the two-gluon exchange picture for these cases. Cases (c) and (d) are hard diffractive processes, and for this situation again the two-gluon exchange picture (with BFKL enhancement if necessary) is appropriate.

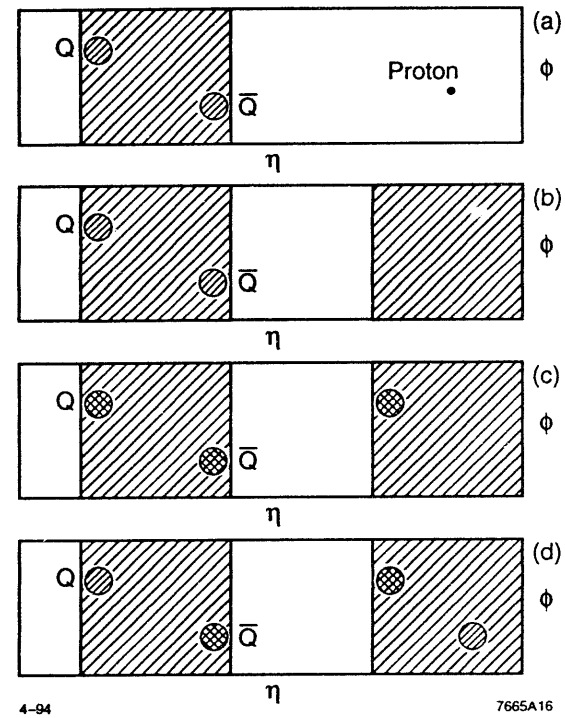

Figure 16. Examples of hard diffraction relevant to HERA. The mechanisms of creation of a dijet from a small $Q\overline{Q}$ color-dipole (a) coherent from the proton, (b) incoherent but soft, (c) incoherent but harder, (d) via a mechanism analogous to that exhibited in Figs. 8 and 11. The lego plots are drawn for reference frames for which the virtual photon and proton are collinear.

We must distinguish whether the momentum-transfer t is large or small compared to Q^2. If t is small, there can be expected to be, for balanced dijets, the suppression of the diffracted final state, as discussed in Section 3 (Eq. (23)). If $t \approx Q^2$ the diffractive cross-section may be small, but the ratio of one-gluon exchange may be enhanced (cf. Eq. (23)).

Most of these cases are already reasonably well-studied by others and in any

case not well-studied by myself. The only additional comment to make here is that in all the cases discussed above, the characteristic mass of the diffracted system (the virtual-photon fragments) is $\lesssim \sqrt{Q^2}$. This will be in contrast to the situation for the structured virtual photon (case 2 in the previous section).

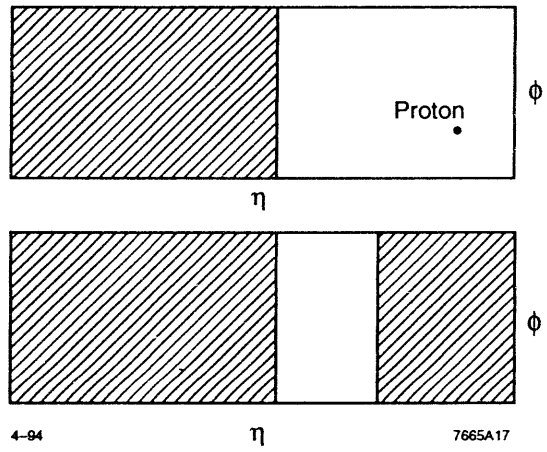

Figure 17. Single and double soft diffraction.

The generic final state for the "not-so-simple" aligned-jet photon configuration is a uniform distribution not too dissimilar from hadron-nucleon scattering. If the virtual-photon is just as opaque as a pion, we could expect diffraction-dissociation, via the non-perturbative "soft-Pomeron" physics, to occur just as often. This happens a large fraction of the time, $\sim 10\%$. The final state, shown in Fig. 17, typically will have a diffracted mass M_x^2 large compared with Q^2; because the gap width is not exponentially suppressed

$$M_X^2 \frac{d\sigma}{dM_X^2} = \frac{d\sigma}{d\eta_{\rm gap}} \approx \text{constant} . \tag{45}$$

However, it is not clear how structured the "aligned-jet" virtual photon really is. But a reasonable guess is that it is as opaque as a *single* constituent quark. The picture is that the slow member of the pair has time to be "fully dressed," while the fast member does not, and acts as a pointlike parton. If this notion is true, one might be able to obtain information on constituent-quark opacity from deep-inelastic scattering from nuclei.

Of this profusion of options for diffractive final states, one discriminant stands out rather clearly:

For the color-dipole, simple "direct" mechanism, the distribution of diffracted masses is peaked near Q^2, while for the aligned jet mechanism it is broader. I would suggest plotting $M_X^2 dN/dM_X^2$ versus M_X^2/Q^2. Here

$$dN = \frac{1}{\sigma}\, d\sigma \tag{46}$$

is differential in other phase space variables as appropriate. If the variable

$$\beta = \frac{Q^2}{M_X^2 + Q^2} \tag{47}$$

is preferred, one might try $\beta dN/d\beta$ versus β instead. The generic behavior for the two cases are sketched in Fig. 18. Especially interesting will be to map the transition from the photoproduction limit, where some soft diffraction should exist, to the BFKL region of $Q^2 \gtrsim 10\ GeV^2$ seen in the HERA data.

It is clear that this field is making great progress both theoretically and experimentally. We can expect major advances in the understanding of the nature of the virtual photon and of hard diffraction in the near future.

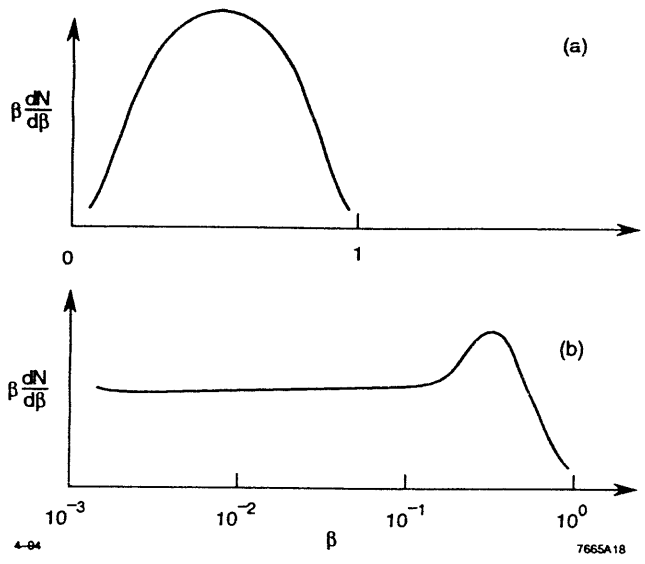

Figure 18. Expected behaviors for (a) the diffractively produced symmetric dijets, and (b) soft non-perturbative diffraction.

REFERENCES

[1] G. Ingelman, discussion comment.

[2] P. Collins and E. Squires, *An Introduction to Regge Theory and High Energy Physics*, Cambridge, University Press, Cambridge (1977). See also J. Bjorken, SLAC-PUB-6463.

[3] A. Donnachie and P. Landshoff, Phys. Lett. **B296**, 227 (1992).

[4] Ya. Balitsky and L. Lipatov, Sov. J. Nucl. Phys. **28**, 822 (1978); E. Kuraev, L. Lipatov, and V. Fadin, Sov. Phys. JETP **45**, 199 (1977).

[5] See for example A. Donnachie, these proceedings.

[6] J. Bjorken, Nucl. Phys. B (Proc. Suppl.) **25B**, 253 (1992); also Acta. Physica Polonica **B23**, 637 (1992).

[7] A. Manohar and H. Georgi, Nucl. Phys. **B234**, 189 (1984).

[8] N. Nikolaev and B. Zakharov, Zeit. Phys. **C49**, 607 (1991); **C53**, 331 (1992).

[9] A. Mueller, Columbia University preprint CU-TP-609 (August 1993).

[10] J. Kogut and D. Soper, Phys. Rev. **D1**, 2901 (1970).

[11] J. Bjorken, J. Kogut, and D. Soper, Phys. Rev. **D3**, 1382 (1971).

[12] The concept of double-sided phase space goes back to G. Veneziano, Phys. Lett. **43B**, 413 (1973). For a detailed exposition of the QCD point of view adopted here, see J. Bjorken, Phys. Rev. **D45**, 4077 (1992).

[13] D. Zeppenfeld, University of Wisconsin preprint MAD-PH-806, November 1993.

[14] J. Bjorken, Phys. Rev. **D47**, 101 (1992); see also SLAC preprint SLAC-PUB-6463 (1994).

[15] The absorption is due to interaction of spectator-partons, which should be absent in the virtual photon under the conditions specified above (see J. Bjorken, Ref. 14; E. Gotsman, E. Levin, and U. Maor, Phys. Lett. **B309**, 199 (1993) for detailed discussions of $\langle |S|^2 \rangle$).

[16] J. Collins, L. Frankfurt, and M. Strikman, Phys. Lett. **B307**, 161 (1993).

[17] A. Donnachie and P. Landshoff, Phys. Lett. **B285**, 172 (1992).

[18] G. Ingelman and P. Schlein, Phys. Lett. **152B**, 256 (1985).

[19] There is some experimental evidence for this; see A. Brandt *et al.*, UA8 Collaboration, Phys. Lett. **B297**, 417 (1992).

[20] N. Nikolaev, B. Zakharov, and V. Zoller, Jülich preprint KFA-IKP(Th)-1993-34 (1993).

[21] A. Mueller and B. Patel, Columbia University preprint CU-TP-625 (1994).

[22] V. Del Duca, Phys. Rev. **D48**, 5133 (1993).

[23] L. Lipatov, University of Padua preprint DFPD/93/TH/70 (October 1993), and these proceedings.

[24] This structure could be anticipated from the known form of exact Parke-Taylor multigluon amplitudes; see V. Del Duca, Ref. 22; S. Parke and T. Taylor, Phys. Rev. Lett. **56**, 2459 (1986).

[25] See, e.g., R. Field, "Applications of Perturbative QCD," Addison-Wesley (New York), 1989; p. 358.

[26] F. Sciulli; these proceedings.

[27] The history goes back a long way. I naturally remember my own involvement in it the best, which began with learning of Gribov's paradox [naive VMD leads to a virtual photon-nucleus cross-section $\approx (\pi R^2) \cdot (3\alpha/\pi)\, \ell n Q^2$] and struggling with its resolution (J. Bjorken, "Particle Physics" (Irvine Conference, 1971), AIP Conference Proceedings No. 6, Particles and Fields Subseries, No. 2, ed. M. Bander, G. Shaw, and D. Wong (AIP, New York, 1972). See also J. Bjorken, "Lecture Notes in Physics, No. 56, Current Induced Reactions," ed. J, Körner, G. Kramer, and D. Schildknecht, Springer-Verlag, Berlin (1976).

[28] See for example J. Bjorken, Ref. 27; also J. Bjorken and J. Kogut, Phys. Rev. **D8**, 1341 (1973).

DATE

FILMED

7/7/94

END